Applied Thermal Engineering 219 (2023) 119434

Contents lists available at ScienceDirect

Applied Thermal Engineering

journal homepage: www.elsevier.com/locate/apthermeng

Research Paper

Performance of spray cooling with vertical surface orientation: An experimental investigation

Linyi Xiang, Xingjian Yu, Tao Hong, Xuan Yang, Bin Xie, Run Hu, Xiaobing Luo *

School of Energy and Power Engineering, Huazhong University of Science and Technology, Wuhan 430074, PR China

ARTICLE INFO

Keywords:
Spray cooling
Vertical surface orientation
Critical heat flux
Dimensionless correlation

ABSTRACT

Spray cooling is a promising thermal management solution for high heat flux applications. Surface orientation is a key parameter of spray cooling performance while vertical surface orientation has been proved to have excellent heat transfer performance. However, key spray parameters regarding the vertical surface spray cooling system have not been comprehensively studied. In this work, a vertical surface spray cooling system is designed and established. The effects of spray volumetric flux, nozzle-to-surface distance, and coolant inlet temperature on the heat transfer characteristics of spray cooling are experimentally investigated. The system shows a magnificent heat dissipation capability as high as a critical heat flux of 596 W/cm^2 at a low spray volumetric flux (0.83 $\times$ 10^{-2} m^3·s^{-1}·m^{-2}). Nozzle-to-surface distance, which has no obvious effect on the two-phase regime, is observed to play a significant role in the single-phase regime. Interestingly, the heat transfer coefficient can be enhanced by increasing the coolant inlet temperature while it will not necessarily lower the surface temperature. Furtherly, an experimental dimensionless correlation of Nusselt number for the single-phase regime is proposed, demonstrating a higher contribution of coolant flow properties to the spray cooling system performance with vertical surface orientation. This work reveals the underlying mechanism of how the key spray parameters impact the performance of the spray cooling system with vertical surface orientation and is expected to facilitate high-heat-flux heat dissipation and provide guidance for the research on spray cooling.

1. Introduction

With the rapid development of electronic devices toward high performance and miniaturization, heat dissipation has increasingly become the prime obstacle to the development of electronic devices due to the high heat flux [1–5]. For instance, the heat flux of insulated gate bipolar transistor (IGBT) modules can be up to 500 W/cm^2 [6], while the heat dissipation technologies such as microchannel, heat pipe, and jet impingement can only remove heat flux up to 312 W/cm^2 [7]. Due to its stronger heat dissipation capability, spray cooling is regarded as a promising candidate for the thermal management of high heat flux electronic devices [8–12]. Surface orientation, which can significantly influence the flow of vapor–liquid mixture and the heat and mass transfer processes, is a key feature to spray cooling system [13,14]. Vertical surface orientation has been proved to lead to better heat dissipation capability compared to the other two typical orientations, upward surface orientation and downward surface orientation [15–20].

Spray cooling system with vertical surface orientation thus has drawn tremendous research interest. The reported studies mainly focus on two types of topics. The first type is investigating the effect of surface orientation on the performance of spray cooling system. For instance, Chen et al. performed spray cooling heat flux measurements with three surface orientations where the highest thermal performance at low temperatures was observed in vertical surface orientation [21]. Zhao et al. observed that in medium-spray volumetric fluxes of 2 $\times$ 10^{-3} to 7.61 $\times$ 10^{-3} m^3·s^{-1}·m^{-2}, the critical heat flux (CHF) of the vertical surface orientation is higher than that of the upward and downward surface orientations [14]. The second type of topic is performance enhancement by exploring the impact of the feature parameters of the vertical surface spray cooling system, such as surface properties, coolant properties, and spray properties. Liu et al. employed the surfaces containing micro-roughness to enhance the heat transfer by 136 % and 288 %, respectively. It was also discovered that heat transfer performance of vertical surface spray cooling increases as the surface roughness increases [22]. Singh et al. studied the effect of different surface types including micro-finned, micro-/nano-coated, and hybrid surface on vertical surface spray cooling, of which the results show that hybrid surface owns at least 360 % enhancement in heat transfer coefficient (h) and 72.9 % in CHF in contrast to the plain surface [23]. Liu et al.

* Corresponding author.
E-mail address: Luoxb@hust.edu.cn (X. Luo).

https://doi.org/10.1016/j.applthermaleng.2022.119434
Received 1 June 2022; Received in revised form 21 September 2022; Accepted 29 September 2022
Available online 5 October 2022

Nomenclature

c_p	specific heat at constant pressure
D	surface diameter
d_{32}	Sauter mean diameter
H	nozzle-to-surface distance
h	heat transfer coefficient
h_{fg}	latent heat of vaporization
k	thermal conductivity
Nu	Nusselt number
ΔP	pressure drop across nozzle
Pr	Prandtl number
$\overline{Q}''$	spray volumetric flux
q	heat flux
q''_{CHF}	critical heat flux
Re	Reynolds number
T	temperature
T_{in}	inlet coolant temperature
T_{sat}	saturation temperature
We	Weber number
y	y coordinate

Greek symbols

η	evaporation efficiency
σ	surface tension
μ	dynamic viscosity
ρ	density

Subscripts

f	liquid
g	vapor; gas
in	inlet
s	spray
sat	saturation
w	surface

Abbreviations

CHF	Critical heat flux
RHS	Replaceable heat source
SMD	Sauter mean diameter

compared the enhancement of spray cooling heat transfer using deionized water with a conventional surfactant (Tween 20) and two biosurfactants (Rhamnolipid and Sophorolipid). They achieved the h as high as 29654 W/m^2·K [24]. These previous studies may provide guidance to the performance enhancement to some extent [25]. However, most of them focus on surface properties and coolant properties, rarely involving spray volumetric flux ($\overline{Q}''$), nozzle-to-surface distance (H), and coolant inlet temperature (T_{in}) [26], which can hardly show comprehensive guidance for the practical application. Besides, a quantitative evaluation framework is still lacking to gauge the performance of a spray cooling system with vertical surface orientation [27,28]. Therefore, the effects of$\overline{Q}''$, H, and T_{in} and a feasible evaluation method are in urgent need of exploration.

In this work, a spray cooling system based on vertical surface orientation is designed, fabricated, and tested with a proposed high heat flux replaceable heat source. In addition, the effect of spray properties such as$\overline{Q}''$, H and T_{in} on the heat transfer performance of vertical surface spray cooling have been revealed. A quantitative evaluation of these effects and a general correlation of Nusselt number (Nu) for single-phase regime has been proposed with deionized water as coolant. Hence, this work reveals the underlying mechanism of how the key spray parameters impact the performance of the spray cooling system with vertical surface orientation and is expected to provide guidance for the performance enhancement of spray cooling system and to facilitate the high-heat-flux heat dissipation in electronic devices.

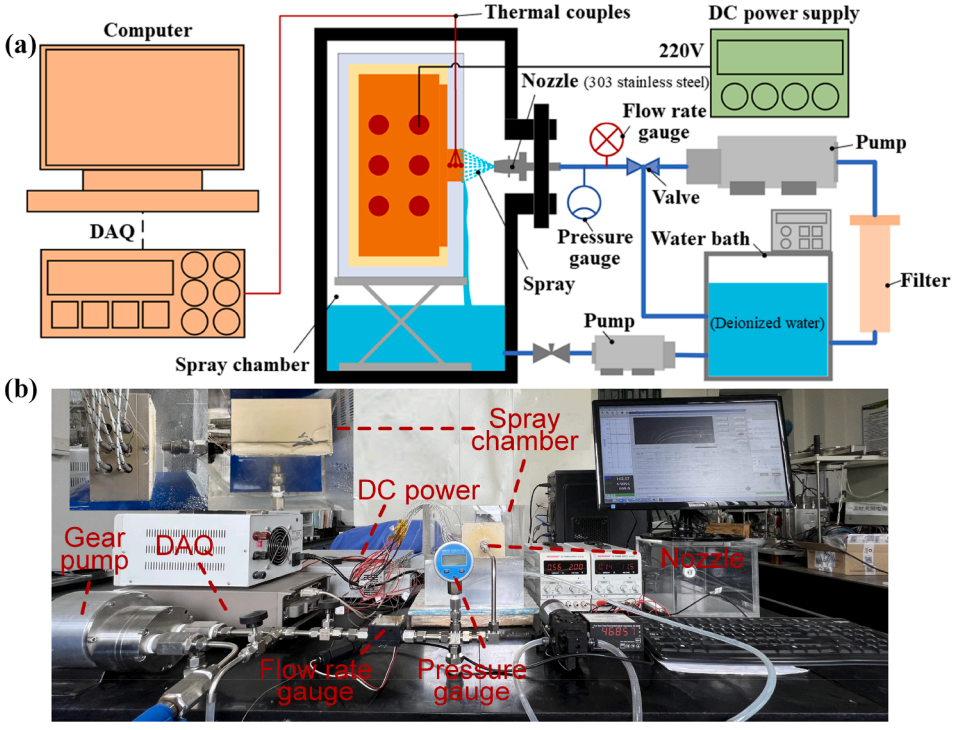

Fig. 1. (a) Schematic of the spray cooling system, (b) Photo of the experimental system.

2. Methods

2.1. Spray cooling system

Fig. 1 shows the schematic diagram and photographic view of the experimental system which consists of five subsystems, including the spray system, the spray chamber, the electrical heating system, the active-based cooling system, and the data acquisition system. The deionized water is stored in a water bath (DC-2010, temperature control range: −20-100℃, accuracy: ±0.1 %, Zhulan) as the working fluid, of which the related parameters can be found in Table S1. And the working fluid is driven into the spray system by a gear pump (NP400 24 V-400 W, Suofu Co., ltd) after passing through a filter (TPP-15, filtration accuracy: 15 μm, Atenjoy). There is a three-way valve at the outlet of the gear pump, and the flow rate of the working fluid is controlled by adjusting the valve opening and the speed of the gear pump. A solid cone pressure nozzle (B1/4TT-SS + TG-SS0.3, Spraying Systems Company) is used for the formation of spray which is made of 303 stainless steel. The heat source module is put in the spray chamber which is made of the transparent acrylic board for observation. After the experiment, the cooling working fluid collected in the spray chamber is driven back to the water bath by the diaphragm pump.

2.2. Replaceable heat source

Fixed heat source would bring difficulties to the maintenance of the heat source in the experiment, which is also far from the application scenario. It is very important to design a heat source which can reflect the operating conditions of the electronic equipment with high power, high heat flux, and small size. In this paper, the replaceable heat source (RHS) is proposed which can be operated independently. The finite element analysis method is used to design the heat source by which three main targets are achieved. Firstly, the size of the heat source is as small as possible. Secondly, the temperature of each part of the heat source does not exceed the affordable temperature of the materials. Last but not least, most of the heat is dissipated from the surface in direct contact with coolant.

The thermal conductivities of the materials used in the numerical simulation are shown in Table 1. The list of boundary conditions and assumptions used in the numerical simulation are as follows:

(1) In spray cooling, the target surface temperature is uniform after cooling. So a constant convective heat transfer coefficient can be applied to the target surface as a boundary condition in the numerical simulation. Here the convective heat transfer coefficient is the average heat transfer coefficient of the target surface.
(2) Heat dissipation of thermal radiation is ignored, and the heat is mainly lost through the surface in direct contact with coolant in the way of convection heat transfer.
(3) The thermal properties (thermal conductivity, heat capacity, and density) of all materials are assumed to be uniform, isotropic, and independent of temperature.
(4) The material contact through the interface is considered perfect (no air gap and surface roughness).

Fig. 2 shows the schematic of RHS, and the framework of RHS is processed by PEEK (Polyether-ether-ketone) (Thermal conductivity: 0.29 W/m·K and operating temperature up to 300℃). The copper block which is made of oxygen-free copper (Thermal conductivity: 398 W/m·K). The framework is fixed by screws and the insulation cotton (Thermal conductivity: 0.03 W/m·K) fills the space between the framework and the copper block. The underside of the copper block is bored to accept six cartridge heaters (220 V 300 W, Xianggui) which provide stable input electrical power by a programmable DC power supply (FTP032-300–16, Faith).

Table 1
Thermal conductivity of materials used in the numerical study.

Material	Materials	Thermal conductivity (W/m·K)
Copper block	Copper	398
Heating rods	Al_2O_3	30
Thermal insulation cotton	Cotton	0.03
PEEK	PEEK	0.29

The copper block is a three-layer round table structure with the diameters of 90 mm, 80 mm, and 16 mm from bottom to top. The heating rod is a cylinder with the diameter of 10 mm and the length of 50 mm. In order to measure the temperature of the copper block, six K-type thermocouples (TT-K-36, ETA) are embedded in RHS, as shown in Fig. 2. Before each experiment, the surface of the copper block is polished by 600 mesh sandpapers and rinsed with deionized water to remove the oxidation layer.

2.3. Measurements and data acquisition system

The$\overline{Q''}$, pressure drop across nozzle (ΔP), and Sauter mean diameter (SMD, d_{32}) are three generally used parameters to assess the performance of spray cooling systems. In our setup, the $\overline{Q''}$ and ΔP are measured by the flow meter (CX-*P*2-F, measuring range: 0.025–2.499 × 10^{-2} $m^3 \cdot s^{-1} \cdot m^{-2}$, accuracy: ±0.5 %, Gnflowmeter) and pressure gauge (SIN-Y190, measuring range: 0–5 MPa, accuracy: ±1%, Sinomeasure) respectively. The SMD is measured by using Sympatec's Laser Diffraction Analyzer. In the measurement of droplet diameter, a R6 camera lens is used (measuring range: 0.5–1750 μm). The whole test system consists of laser transmitter, receiver, and data analysis workstation. The laser transmitter emits a laser stroke to analyze the cross-section. When the droplet passes through the cross-section, the droplet cuts the laser light. The scattering angle and light intensity formed by droplets of different sizes are different. The laser receiver receives and analyzes the scattering angle and light intensity of the laser after being cut by the droplet, and finally obtains the particle size distribution of the droplet through analysis. The performance of the nozzle has been shown in Fig. 3, including the relationship between SMD and$\overline{Q''}$, SMD and *H*, and ΔP and$\overline{Q''}$.

In addition, K-type thermocouples are embedded in the water bath, spray chamber, and inside the copper block to measure the coolant temperature at the nozzle outlet and ambient temperature, and to prevent the RHS from thermal destruction. A data acquisition instrument (Keithley 2700) is used to collect and record the signals of all thermocouples and displays them in real time on the computer.

2.4. Data analysis method and uncertainty analysis

In this work, the heat flux (q) is determined from the uniform temperature gradient between a series of thermocouples in the copper block which can be proved by Fig. S1 and Fig. S2, and the one-dimensional Fourier's law of heat conduction can be applied as:

$$q = -k\frac{\Delta T(y)}{\Delta y} \tag{1}$$

Moreover, the temperature of target surface T_w and h can be calculated as:

$$T_w = T_3 + y_3\frac{\Delta T(y)}{\Delta y} \tag{2}$$

$$h = \frac{q}{(T_w - T_{in})} \tag{3}$$

As shown in Fig. 2, T_3 is the furthest thermocouple from the surface impacted by the spray which is more stable and accurate. Therefore, T_3 is chosen as the base point temperature to obtain the T_w in Eq. (2).

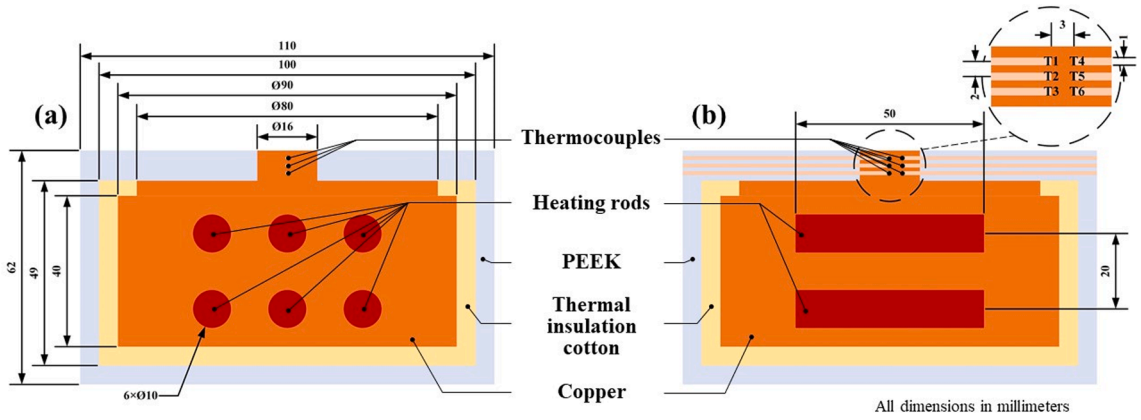

Fig. 2. Sectional diagram of the heat source, (a) The view perpendicular to the heating rods, (b) The view parallel to the heating rods.

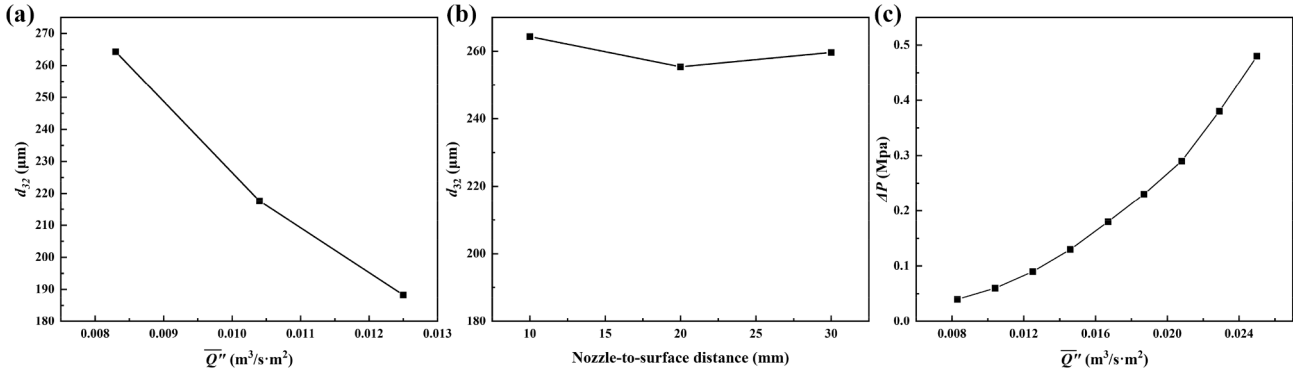

Fig. 3. Performance of nozzle, (a) Sauter mean diameter SMD versus spray volumetric flux$\overline{Q''}$, (b) Sauter mean diameter SMD versus nozzle-to-surface distance H, (c) Pressure drop across nozzle ΔP versus spray volumetric flux$\overline{Q''}$.

In the process of applying one-dimensional Fourier's law, the direct measurement error and the instrumental error are taken into consideration and converted into indirect variable uncertainties. The uncertainties of the K-type thermocouple, fitted slope of three thermocouples, and distance between thermocouples are about ± 0.8℃, ±0.01, and ± 0.1 mm.

Based on error transfer functions on this experimental bench, the uncertainties of surface temperature, heat flux, and heat transfer coefficient can be calculated by [29]:

$$\sigma_y = \sqrt{\sum_{i=1}^{n} \left(\frac{\partial f}{\partial x_i}\right)^2 \sigma_{x_i}^2} \tag{4}$$

The results showed that the average uncertainties of surface temperature, heat flux, and heat transfer coefficient are ± 4.1, ±6.7, and ± 4 %, respectively.

3. Results and discussion

In order to study the influence of spray volumetric flux ($\overline{Q''}$), nozzle-to-surface distance (H), and coolant inlet temperature (T_{in}) on the performance of our spray cooling system, a series of experiments are conducted with the heat flux (q) increases from 0 W/cm^2 to CHF.

3.1. Boiling curve of spray cooling

The cooling boiling curve is shown in Fig. 4, which has three stages, namely, the single-phase regime, the transition regime, and the two-phase regime. In the single-phase regime, the increase of h is relatively slow and dissipation of heat in this stage is mainly dependent on the sensible heat of the coolant. In the transition regime, due to the temperature of the heating surface being close to the saturation temperature of the coolant, the phase change of a small part of the coolant happened and the curve is oscillating. In the two-phase regime, with the increase of q, the h increases sharply due to the phase change of most of the coolant.

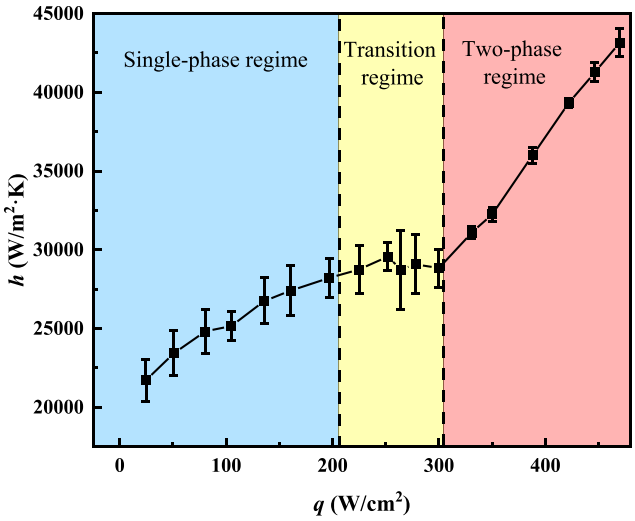

Fig. 4. Cooling boiling curve of spray cooling with the $\overline{Q''}$ of 0.83 × 10^{-2} m^3·s^{-1}·m^{-2}.

3.2. Effects of spray volumetric flux

Three different $\overline{Q''}$ of 0.83 × 10^{-2} $m^3{\cdot}s^{-1}{\cdot}m^{-2}$, 1.04 × 10^{-2} $m^3{\cdot}s^{-1}{\cdot}m^{-2}$ and 1.25 × 10^{-2} $m^3{\cdot}s^{-1}{\cdot}m^{-2}$ are chosen and tested based on the same H (10 mm) and T_{in} (25℃). The relationship between h and q at different $\overline{Q''}$ and the relationship between q and temperature difference at different $\overline{Q''}$ are displayed in Fig. 5.

It can be found that the h increases with the $\overline{Q''}$ in Fig. 5a. Here, with $\overline{Q''}$ goes from 0.83 × 10^{-2} to 1.04 × 10^{-2} and to 1.25 × 10^{-2} $m^3{\cdot}s^{-1}{\cdot}m^{-2}$, it can be seen that the highest h increases from 43159 W/m^2·K to 46348 W/m^2·K and then to 47156 W/m^2·K. Moreover, when the T_w approaches the saturation temperature of the coolant, there is no transition from the single-phase regime to the two-phase regime when $\overline{Q''}$ are 1.04 × 10^{-2} and 1.25 × 10^{-2} $m^3{\cdot}s^{-1}{\cdot}m^{-2}$. As the result, the h of 0.83 × 10^{-2} $m^3{\cdot}s^{-1}{\cdot}m^{-2}$ exceeds the h of 1.04 × 10^{-2} $m^3{\cdot}s^{-1}{\cdot}m^{-2}$ when q varies from 408 to 469 W/cm^2. This is because that although the increase in $\overline{Q''}$ leads to a more effective forced convection heat transfer due to the faster speed of liquid film, the liquid film gets thicker at larger$\overline{Q''}$. The thicker liquid film will significantly inhibit the evaporation of the liquid film. Because of the greater magnitude of the latent heat (in evaporation) as compared to the sensible heat (in forced convection), the heat transfer increases steeply.

Fig. 5b exhibits the q versus temperature difference T_w-T_{in} at different$\overline{Q''}$. T_w-T_{in} varies from ~ 10 to ~ 120℃ with the q ranging from ~ 20 to ~ 570 W/cm^2. The trends of the curves imply that higher h results in lower surface temperature under the same heat flux. Specifically, with a very high heat flux of 300 W/cm^2, the temperature difference T_w-T_{in} is lower than 95℃ which means T_w can be controlled below 120℃, a safe working temperature of electronic equipment, since the inlet coolant temperature is 25℃.

The SMD of droplets at different $\overline{Q''}$ is analyzed by LDA. As shown in Fig. 3a, the results show that with the increase of$\overline{Q''}$, the SMD becomes smaller when droplets reach the surface. When $\overline{Q''}$ increases from 0.83 × 10^{-2} to 1.25 × 10^{-2} $m^3{\cdot}s^{-1}{\cdot}m^{-2}$, the SMD reduces from 264 to 188 μm, a 30 % reduction. The smaller SMD facilitates heat transfer on high-temperature surfaces, thereby improving the effectiveness of spray cooling.

As a result, the single-phase heat transfer coefficients at $\overline{Q''}$ of 1.04 × 10^{-2} and 1.25 × 10^{-2} $m^3{\cdot}s^{-1}{\cdot}m^{-2}$ exceed the two-phase heat transfer coefficient at $\overline{Q''}$ of 0.83 × 10^{-2} $m^3{\cdot}s^{-1}{\cdot}m^{-2}$ when the q is the same. It can be seen that $\overline{Q''}$ is critical for spray cooling for more coolant and smaller droplet size.

3.3. Effects of nozzle-to-surface distance

Fig. 6a compares the effect of H on the heat transfer performance of spray cooling in the single-phase and the two-phase regimes based on the same $\overline{Q''}$ (0.83 × 10^{-2} $m^3{\cdot}s^{-1}{\cdot}m^{-2}$) and T_{in} (25℃). Fig. 6b shows the q versus the temperature difference between surface temperature and coolant inlet temperature at different H.

It can be seen from Fig. 6a that in the single-phase regime, the larger the H, the lower the h. When H increases from 10 mm to 30 mm in the single-phase regime, the highest h decreases from 43159 W/m^2·K to 35040 W/m^2·K. Moreover, with the increase of q, h at three different H are similar in the two-phase regime, and the slopes are also very close. At the same time, it can be seen that H can make up for the low h of the single-phase regime compared with the two-phase regime due to the different heat transfer mechanism. For example, as the heat flux of 200 W/cm^2, the h is 28213 W/m^2·K in the single-phase regime when H is 10 mm while h are 22274 W/m^2·K and 20517 W/m^2·K when H are 20 mm and 30 mm, which had entered the two-phase regime, and the enhancement ratios are 27 % and 38 %, respectively.

Fig. 6b shows that in the single-phase regime, under the same q, the larger the H, the higher the surface temperature. As mentioned before, forced convection heat transfer and evaporation heat transfer are the main mechanisms of single-phase regime. As the distance decreases, the perturbation of the liquid film by the droplet is stronger and more frequent, enhancing the convection heat transfer. At the same time, faster flow velocity of the liquid film, thinner liquid film, and higher temperature of the liquid film will intensify the evaporation heat transfer. Therefore, the heat transfer at low H is stronger.

The SMD of droplets at different H are shown in Fig. 3b. The results show that the SMD does not change with H obviously, which means it is not the main factor influencing the performance of the spray cooling in this situation.

3.4. Effects of coolant inlet temperature

Fig. 7a compares the effect of T_{in} on the performance of spray cooling in the single-phase and two-phase regimes. Under the same input electrical power, $\overline{Q''}$ (0.83 × 10^{-2} $m^3{\cdot}s^{-1}{\cdot}m^{-2}$) and H (10 mm), the higher the T_{in}, the greater the h. The highest h reaches 44356 W/m^2·K as T_{in} is 35℃, 43159 W/m^2·K as T_{in} is 25℃ and 39588 W/m^2·K as T_{in} is 15℃. The h at T_{in} of 35 °C increased by 12 % compared with that at T_{in} of 15 °C. On the one hand, the higher the T_{in}, the higher the evaporation rate near the nozzle outlet, which increases the disturbance of the space near the heating surface and strengthens the heat transfer. On the other hand, the higher T_{in} will promote the evaporation of liquid film on the heating

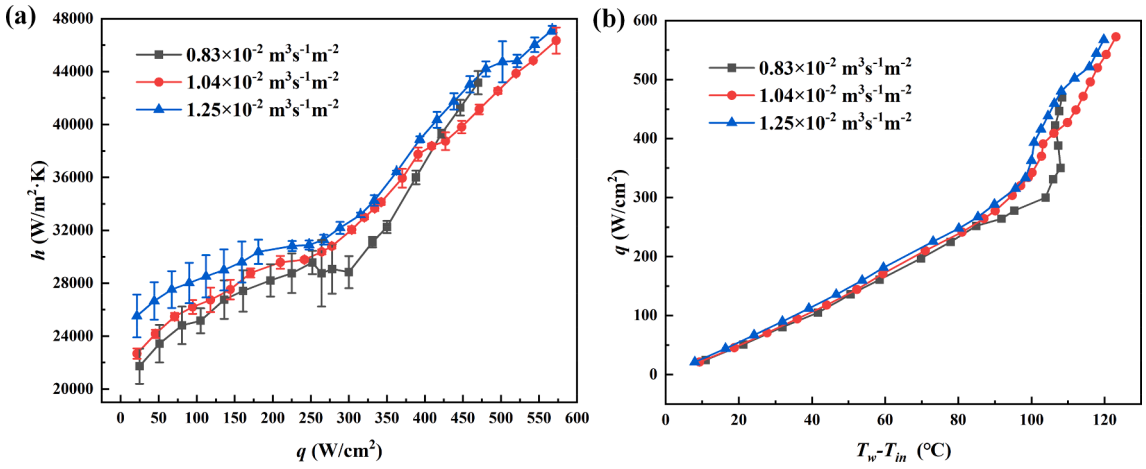

Fig. 5. (a) Heat transfer coefficient h versus heat flux q at different spray volumetric flux$\overline{Q''}$, (b) Heat flux q versus temperature difference T_w-T_{in} at different spray volumetric flux$\overline{Q''}$.

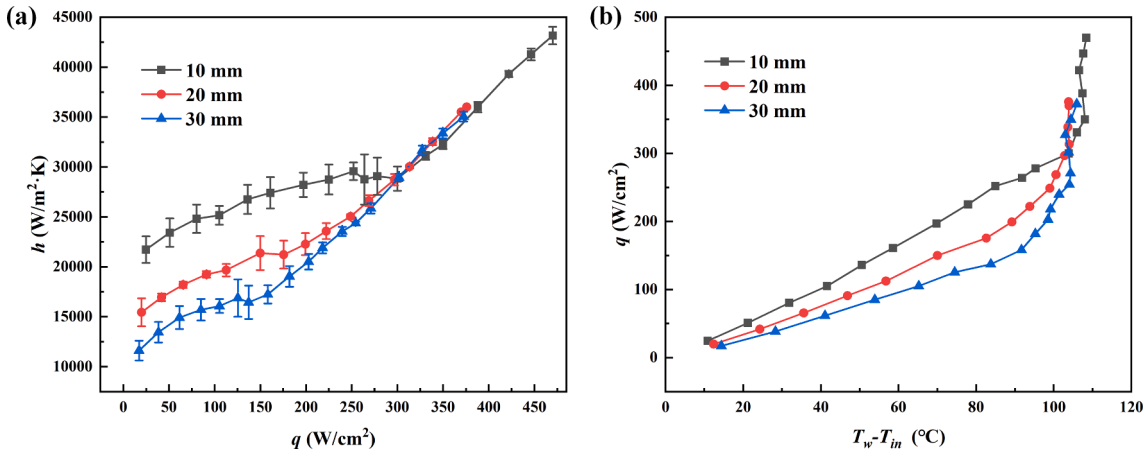

Fig. 6. (a) Heat transfer coefficient h versus heat flux at different nozzle-to-surface distance H, (b) Heat flux versus temperature difference T_w-T_{in} at different nozzle-to-surface distance H.

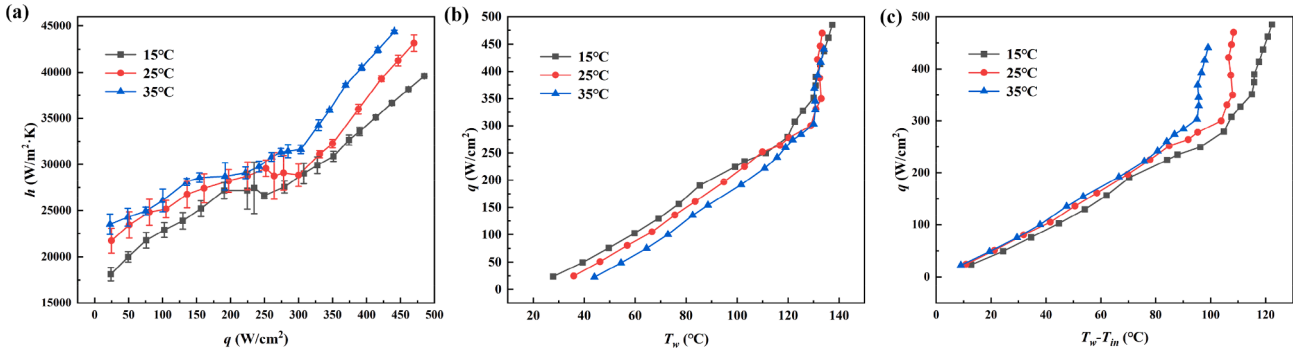

Fig. 7. (a) Heat transfer coefficient h versus heat flux q at different coolant inlet temperature T_{in}, (b) Heat flux q versus surface temperature T_w at different coolant inlet temperature T_{in}, (c) Heat flux q versus temperature difference T_w-T_{in} at different coolant inlet temperature T_{in}.

surface, which tends to the release of latent heat of coolant.

However, the results also show that the increase of T_{in} is not sufficient to enhance the heat transfer in essence, *i.e.*, the high h does not result in a low surface temperature, as shown in Fig. 7b. It can be seen that the surface temperature increases with T_{in} under the same q in the single-phase regime, while there is no obvious difference of surface temperature under different T_{in} in the two-phase regime. On the other hand, the temperature difference between T_w and T_{in} decreases when T_{in} increases, as shown in Fig. 7c. The results explain why the surface temperature increases when the h increases, and it also proves that the performance of spray cooling is affected by many parameters.

3.5. Critical heat flux and evaporation efficiency

CHF is an important parameter which has been widely used to evaluate the performance of spray cooling. Fig. 8a illustrates CHF versus *We* which is defined as.

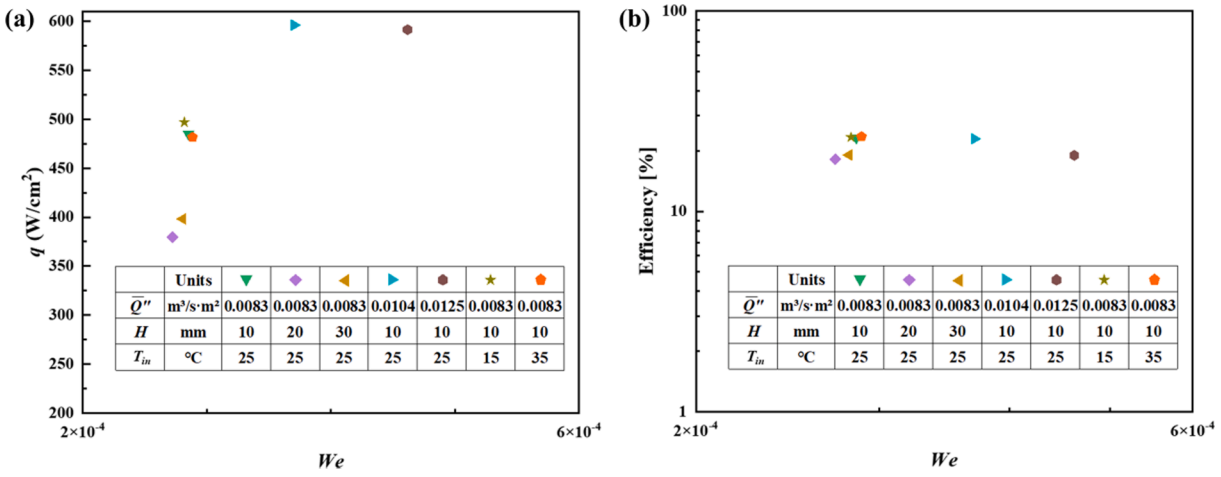

Fig. 8. (a) Critical heat flux CHF versus *We*, (b) Evaporation efficiency versus *We*.

$$We = \frac{\rho_f d_{32} \overline{Q''}^2}{\sigma} \tag{5}$$

As shown in Fig. 8b, another crucial parameter of spray cooling that is related to CHF is evaporation efficiency, η, which is defined as the percentage of the total heat rate that can be removed by the spray, sensible heat and latent heat, to that is removed at CHF [30],

$$\eta = \frac{q''_{CHF}}{\rho_f \overline{Q''}[h_{fg} + c_{p,f}(T_{sat} - T_{in})]} \times 100\% \tag{6}$$

The result shows that the larger the$\overline{Q''}$, the higher the CHF. And there is no noticeable difference between the CHF of 1.04 × 10^{-2} and 1.25 × 10^{-2} $m^3 \cdot s^{-1} \cdot m^{-2}$. It can also be found that the larger the H, the lower the CHF. And the CHF is similar at the H of 20 and 30 mm. The CHF decreases slightly with the increase of T_{in}. CHF reaches as high as 596 W/cm^2 when $\overline{Q''}$ is 0.83 × 10^{-2} $m^3 \cdot s^{-1} \cdot m^{-2}$, H is 10 mm, and T_{in} is 35℃, which has exceeded the highest reported value, 539 W/cm^2, among the systems with same surface orientation and coolant [14]. As Fig. 8b shows, the evaporation efficiency is around 20 % under different working conditions, and it reaches the highest value of 24 % when $\overline{Q''}$ is 0.83 × 10^{-2} $m^3 \cdot s^{-1} \cdot m^{-2}$, H is 10 mm, and T_{in} is 35℃.

4. Heat transfer model and prediction for vertical surface orientation

Due to the complexity of spray cooling process, empirical models have been developed to guide the design of spray cooling systems and applications. There are three different forms of single-phase heat transfer correlations: (a) Nusselt number correlations based on droplet diameter, (b) Nusselt number correlations based on surface size, and (c) direct heat transfer coefficient correlations [9]. In this work, the first form is chosen based on the heat transfer experimental data and spray parameter measurement.

Moreover, it was proved that the liquid film plays an important role in the heat transfer performance of spray cooling systems according to the visualization work of Shedd et al. [31] and Horacek et al [32]. The velocity boundary layer, temperature boundary layer, and the flow regime (laminar or turbulent) are very important to characterizing the heat transfer. Therefore, Reynolds number (Re), which reflects the flow regime, and Prandtl number (Pr), which reflects the relation of velocity and temperature boundary layers, are often used to fit the Nusselt number (Nu) [33].

Under different working conditions, the data for the single-phase regime are fitted by [9].

$$Nu = 1.2 Re_s^{0.96} Pr_f^{0.5} \tag{7}$$

The three dimensionless parameters in Eq. (7) are defined as.

$$Nu = \frac{h d_{32}}{k_f} \tag{8}$$

$$Re_s = \frac{\rho_f \overline{Q''} d_{32}}{\mu_f} \tag{9}$$

$$Pr_f = \frac{c_{p,f} \mu_f}{k_f} \tag{10}$$

where spray volumetric flux and Sauter mean diameter are used as velocity and length scales, respectively. All liquid properties are evaluated under the average of surface and liquid temperatures,$(T_w + T_f)/2$.

Fig. 9 shows the fitting formula and experimental results, where the maximum deviation is 25 %. More specifically, the exponent of 0.96 in the fitting formula is distinctly higher than 0.78, the up-to-date highest reported value, which means Re has a more important effect on heat transfer performance of vertical surface spray cooling system compared to other correlations with upward surface orientation and downward surface orientation [34,35]. On the other hand, coolant flow properties such as the spray volumetric flux and the size of the droplet are significant to spray cooling with vertical surface orientation.

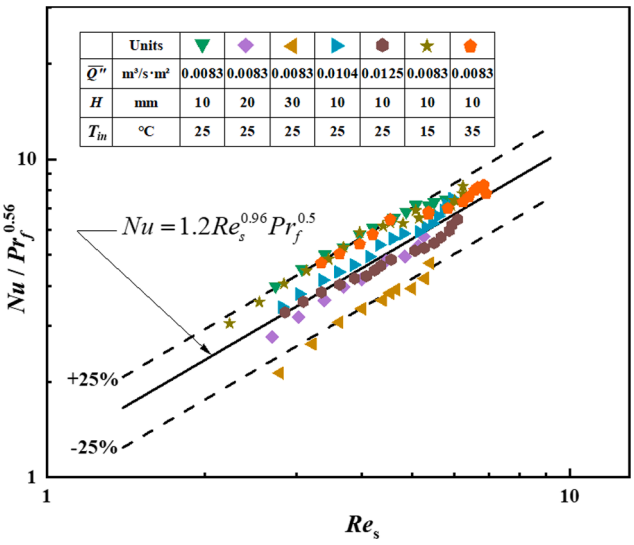

Fig. 9. Nusselt number Nu as a function of Reynolds number Re_s in different working conditions.

5. Conclusion

Experiments have been performed to improve the understanding of the effects of different spray parameters on spray cooling with vertical surface orientation. The results show that spray volumetric flux, nozzle-to-surface distance, and inlet coolant temperature have different effects on the performance of spray cooling. Higher spray volumetric flux results in better heat transfer performance in both the single-phase regime and the two-phase regime. It is observed that the nozzle-to-surface distance mainly influences the performance in the single-phase regime. Significant improvement in heat transfer coefficient has been observed by increasing the inlet coolant temperature while it will not result in a low surface temperature. The performance of our system has furtherly been examined. The maximum critical heat flux obtained at $\overline{Q''}$ of 0.83 × 10^{-2} $m^3 \cdot s^{-1} \cdot m^{-2}$, H of 10 mm, and T_{in} of 35℃ is 596 W/cm^2, the up-to-date highest reported value for vertical surface orientation with the coolant of deionized water. Evaporation efficiency ranges from 19 % to 24 %. Simultaneously, a general correlation is proposed, which proves that coolant flow properties play a more important role in the vertical surface orientation than in other orientations.

CRediT authorship contribution statement

Linyi Xiang: Conceptualization, Methodology, Software, Formal analysis, Investigation, Writing – original draft, Writing – review & editing. **Xingjian Yu:** Conceptualization, Investigation, Writing – review & editing. **Tao Hong:** Methodology, Resources. **Xuan Yang:** Software, Validation. **Bin Xie:** Resources, Writing – review & editing. **Run Hu:** Writing – review & editing. **Xiaobing Luo:** Project administration, Funding acquisition, Writing – review & editing.

Declaration of Competing Interest

The authors declare that they have no known competing financial interests or personal relationships that could have appeared to influence the work reported in this paper.

Data availability

Data will be made available on request.

Acknowledgement

This research is supported by the National Natural Science Foundation of China (51625601).

Appendix A. Supplementary material

Supplementary data to this article can be found online at https://doi.org/10.1016/j.applthermaleng.2022.119434.

References

[1] R.K. Wu, Y.W. Fan, T. Hong, H. Zou, R. Hu, X.B. Luo, An immersed jet array impingement cooling device with distributed returns for direct body liquid cooling of high power electronics, Appl. Therm. Eng. 162 (2019), 114259.
[2] J.X. Wang, Y.Z. Li, Y. Zhang, J.X. Li, Y.F. Mao, X.W. Ning, A hybrid cooling system combining self-adaptive single-phase mechanically pumped fluid loop and gravity-immune two-phase spray module, Int. J. Heat Mass Transf. 176 (2018) 194–208.
[3] X.B. Luo, R. Hu, S. Liu, K. Wang, Heat and fluid flow in high-power LED packaging and applications, Prog. Energy Combust. Sci. 56 (2016) 1–32.
[4] R.G. Mertens, L. Chow, K.B. Sundaram, R.B. Cregger, D.P. Rini, L. Turek, B. A. Saarloos, Spray Cooling of IGBT Devices, ASME. J. Electron. Packag. 129 (3) (2007) 316–323.
[5] J.X. Wang, W. Guo, K. Xiong, S.N. Wang, Review of aerospace-oriented spray cooling technology, Prog. Aerosp. Sci. 116 (2020), 100635.
[6] C. Qian, A.M. Gheitaghy, J. Fan, H. Tang, B. Sun, H. Ye, G. Zhang, Thermal Management on IGBT Power Electronic Devices and Modules, IEEE Access 6 (2018) 12868–12884.
[7] F.R. Siddiqui, C.Y. Tso, H.H. Qiu, C.Y.H. Chao, S.C. Fu, Hybrid nanofluid spray cooling performance and its residue surface effects: Toward thermal management of high heat flux devices, Appl. Therm. Eng. 211 (2022), 118454.
[8] P. Smakulski, S. Pietrowicz, A review of the capabilities of high heat flux removal by porous materials, microchannels and spray cooling techniques, Appl. Therm. Eng. 104 (2016) 636–646.
[9] G.T. Liang, I. Mudawar, Review of spray cooling- Part 1: Single-phase and nucleate boiling regimes, and critical heat flux, Int. J. Heat Mass Transf. 115 (2017) 1174–1205.
[10] S. Khandekar, G. Sahu, K. Muralidhar, E.Y. Gatapova, O.A. Kabov, R. Hu, X. Luo, L. Zhao, Cooling of high-power LEDs by liquid sprays: Challenges and prospects, Appl. Therm. Eng. 184 (2021) 115640.
[11] H.H. Dong, L. Ruan, Y. Wang, J. Yang, F.H. Liu, S.Q. Guo, Performance of air/spray cooling system for large-capacity and high-power-density motors, Appl. Therm. Eng. 192 (2021), 116925.
[12] A. Sarmadian, J.F. Dunne, J.T. Jose, C.A. Long, J.P. Pirault, Temperature control of vibrating heat-generating hardware using spray evaporative cooling in the nucleate boiling region, Appl. Therm. Eng. 200 (2022), 117710.
[13] K. Yoshida, Y. Abe, T. Oka, Y.H. Mori, A. Nagashima, Spray cooling under reduced gravity condition, J. Heat Transf. 123 (2001) 309–318.
[14] X. Zhao, B. Zhang, Z. Yang, Y. Zhao, Surface orientation effects on heat transfer performance of spray cooling, Int. J. Heat Mass Transf. 147 (2020), 118960.
[15] I. Mudawar, Recent advances in high-flux, two-phase thermal management, J. Thermal Sci. Eng. Appl. 5 (2013), 021012.
[16] L.J. Elston, K.L. Yerkes, S.K. Thomas, J. McQuillen, Cooling performance of a 16-nozzle array in variable gravity, J. Thermophys. Heat Transfer 23 (3) (2009) 571–581.
[17] B. Liu, B. Yuan, P. Z. Xu, J. F. Zhao, Y. H. Zhang, J. J. Wei, Y. Y, Q. Cao, A method for approximating the CHF of subcooled flow boiling in microgravity by ground tests, Int. J. Multiphase Flow, 122 (2020) 103161.
[18] N.Y. Zhou, F.J. Chen, Y.C. Cao, M.M. Chen, Y. Wang, Experimental investigation on the performance of a water spray cooling system, Appl. Therm. Eng. 112 (2017) 1117–1128.
[19] C.-C. Hsieh, S.-C. Yao, Evaporative heat transfer characteristics of a water spray on micro-structured silicon surfaces, Int. J. Heat Mass Transf. 49 (5-6) (2006) 962–974.
[20] K.J. Choi, S.C. Yao, Mechanism of film boiling heat transfer of normally impacting spray, Int. J. Heat Mass Transf. 30 (1987) 311–318.
[21] D.F. Chen, D.W. Tang, X.G. Hu, Effect of microgrooved surface and surface orientation on spray cooling heat transfer, Proceedings of the ASME 2009 International Mechanical Engineering Congress and Exposition 9 (2009) 1555-1561.
[22] P.F. Liu, R. Kandasamy, J.Y. Ho, J.L. Xie, T.N. Wong, Experimental study on heat transfer enhancement using combined surface roughening and macro-structures in a confined double-nozzle spray cooling system, Appl. Therm. Eng. 202 (2022), 117850.
[23] S. Singh, R. Kukreja, Experimental study on effect of enhanced surfaces and inclined mode on spray cooling heat transfer performance using HFE-649 coolant, Energy Sources Part A 44 (3) (2022) 6537–6555.
[24] P.F. Liu, R. Kandasamy, J.Y. Ho, H.C. Feng, T.N. Wong, Comparative study on the enhancement of spray cooling heat transfer using conventional and bio-surfactants, Appl. Therm. Eng. 194 (2021), 117047.
[25] Z.F. Zhou, B. Chen, Y.S. Wang, L.J. Guo, G.X. Wang, An experimental study on pulsed spray cooling with refrigerant R-404a in laser surgery, Appl. Therm. Eng. 39 (2012) 29–36.
[26] Z.B. Yan, K.C. Toh, F. Duan, T.N. Wong, K.F. Choo, P.K. Chan, Y.S. Chua, Experimental study of impingement spray cooling for high power devices, Appl. Therm. Eng. 30 (10) (2010) 1225–1230.
[27] J. Wang, Y.Z. Li, J. Wang, Transient performance and intelligent combination control of a novel spray cooling loop system, Chinese J. Aeronaut. 26 (5) (2013) 1173–1181.
[28] G.T. Liang, I. Mudawar, Review of spray cooling– Part 2: High temperature boiling regimes and quenching applications, Int. J. Heat Mass Transf. 115 (2017) 1206–1222.
[29] R.J. Moffat, contributions to the theory of single-sample uncertainty analysis, J. Fluids Eng. 104 (1982) 250–258.
[30] K.A. Estes, I. Mudawar, Correlation of Sauter mean diameter and critical heat flux for spray cooling of small surfaces, Int. J. Heat Mass Transf. 38 (16) (1995) 2985–2996.
[31] T.A. Shedd, A.G. Pautsch, Spray Impingement Cooling with Single- and Multiple-Nozzle Arrays, Part II: Visualization and Empirical Models, Int. J. Heat Mass Transf. 48 (15) (2005) 3176–3184.
[32] B. Horacek, K.T. Kiger, J. Kim, Single Nozzle Spray Cooling Heat Transfer Mechanisms, Int. J. Heat Mass Transf. 48 (8) (2005) 1425–1438.
[33] T.A. Shedd, Next Generation Spray Cooling: High Heat Flux Management in Compact Spaces, Heat Transfer Eng. 28 (2) (2007) 87–92.
[34] J.R. Rybicki, I. Mudawar, Single-phase and two-phase cooling characteristics of upward-facing and downward-facing sprays, Int. J. Heat Mass Transf. 49 (1-2) (2006) 5–16.
[35] I. Mudawar, W.S. Valentine, Determination of the local quench curve for spray-cooled metallic surfaces, J. Heat. Treat. 7 (2) (1989) 107–121.